Piezoelectric Polymers Actuators for Precise Shape Control of Large Scale Space Antennas

Qin Chen, Don Natale, Bret Neese, Kailiang Ren, Minren Lin, and Q. M. Zhang
Electrical Engineering Department and Materials Research Institute
The Penn State University, University Park, PA 16802

Matthew Pattom, K. W. Wang
Structural Dynamics and Controls Lab
Department of Mechanical and Nuclear Engineering
The Penn State University, University Park, PA 16802

Houfei Fang, Eastwood Im
Jet Propulsion Laboratory
California Institute of Technology, Pasadena, CA 91109-8099

ABSTRACT

Extremely large, lightweight, in-space deployable active and passive microwave antennas are demanded by future space missions. This paper investigates the development of PVDF based piezopolymer actuators for controlling the surface accuracy of a membrane reflector. Uniaxially stretched PVDF films were poled using an electrodeless method which yielded high quality poled piezofilms required for this application. To further improve the piezoperformance of piezopolymers, several PVDF based copolymers were examined. It was found that one of them exhibits nearly three times improvement in the in-plane piezoresponse compared with PVDF and P(VDF-TrFE) piezopolymers. Preliminary experimental results indicate that these flexible actuators are very promising in controlling precisely the shape of the space reflectors. To evaluate quantitatively the effectiveness of these PVDF based piezopolymer actuators for space reflector applications, an analytical approach has been established to study the performance of the coupled actuator-reflector-control system. This approach includes the integration of a membrane reflector model, PVDF piezopolymer actuator model, solution method, and shape control law. The reflective Newton method was employed to determine the optimal electric field for a given actuator configuration and loading/shape error.

Keywords: deployable antenna, shape control, electroactive polymers (EAP), actuator, piezoelectric

1 INTRODUCTION

In-space microwave antennas experience shape deviations due to pre-stress and thermal expansion. In order to maintain the desired shape of the antenna reflector, it is necessary to have a real-time control system monitor and adjust the surface profile of the reflector. Figure 1 shows the schematic of this high-precision antenna surface control system. Major components of this system include a thin-material reflector, a wavefront sensor, a controller, actuators, and corresponding power amplifier and signal conditioning electronics. Actuators are attached to the back of the reflector to produce contraction/expansion forces to adjust the shape of the thin-material reflector. The metrology

system continuously measures the surface figure of the reflector, converts the surface figure to digital data, and feeds the data to the controller. The controller determines the control parameters and generates commands to the actuator system through the corresponding power amplifiers. The flexible PVDF film actuators are thus activated, which provide the control forces needed to correct any distortions exist in the reflector surface. Future reflectors will be composed of very thin (only several mil thick) materials, and hence the actuator has to be very thin (one to two mil) and very flexible. Currently available PZT based actuators are not applicable for this application. An innovative actuator technology, namely flexible PVDF film actuator technology, has been developed and demonstrated in this study. This technology is extremely suitable and highly effective in controlling the surface precision for large, extra lightweight thin-material antenna reflectors. The successful development of this high-precision antenna surface control system will dramatically improve the resolution of space-based reconnaissance of phenomena of potential intelligence value in anywhere and at anytime. Besides RF applications, this technology is also readily applicable to optical applications such as nano-laminate mirrors and thin film mirrors.

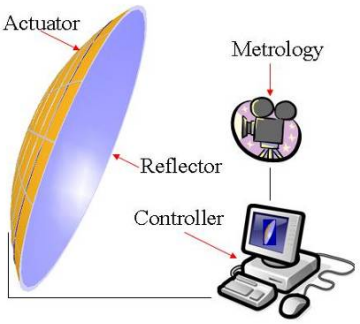

In this paper, an analytical model is first presented to study the performance of the control system. The development of fabrication processes for PVDF actuators is then described. The feasibility of using novel electroactive polymers to obtain more control authority is also discussed. Finally, a prototype membrane reflector is demonstrated and the performance of shape control system is investigated both numerically and experimentally.

2 THEORETICAL ANALYSIS OF THE REFLECTOR SHAPE CONTROL SYSTEM

To facilitate design and analysis and to assess the effectiveness of the PVDF actuator control system for high-precision reflector surface control, an analytical approach has been established. An integrated membrane reflector - PVDF actuator model was developed and solved using the Ritz method, a shape control law was derived, and finally case studies were performed. In this paper, the efforts and results are highlighted. For more detailed discussions, one can refer to [Pattom, 2006] [1].

The reflector and actuators are modeled using a spherical coordinate system. Simply-supported boundary conditions at the rim and pre-stress due to internal inflation pressure are assumed for the reflector. Strain energy was formulated to derive the system model equations and solved using the Ritz method with the given boundary conditions.

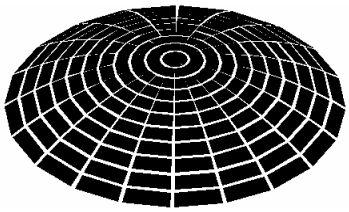

Figure 2. PVDF actuator configuration – 11 rings & 20 rays.

In this investigation, the shape control law is designed based on a least-square (LS) approach. The algorithm used to determine the optimal electric field for a given actuator configuration and loading/shape error is the reflective Newton method. The PVDF material can retain its piezoelectric properties only up to a certain value of the electric field. Beyond this value, it will become depoled (loses its piezoelectric properties). This threshold value determines the limits on the electric field used in the algorithm. The electric fields are determined by minimizing an objective function reflecting the surface displacement error, using the least-squares method while keeping the electric fields within the selected bounds.

Several case studies were performed to investigate the performance of the high-precision large membrane antenna surface control system with the PVDF film actuator. These studies explored the correction of two aspects

of shape distortions that a membrane reflector would experience in space. The first one is the W-error and the second one is due to the thermal loading. When the reflector is inflated, it does not form a perfect spherical shape. The difference between the inflated shape and desired spherical shape is called the 'W-error' [2]. Thermal loading is introduced by temperature change due to solar heating and earth shadowing while the reflector is orbiting.

The material and structural parameters used in this study are listed in Tables 1-3. The PVDF actuator configuration is an arrangement of 11 rings and 20 rays (a total of 220 patches), with complete reflector surface coverage, as shown in Figure 2.

Table 1: Reflector properties.

Dimensions		Material Properties (Kapton®)	
Radius of Curvature (m)	56	Density	$\rho = 1420$ kg/m^3
Diameter (m)	35	Elastic Modulus	$E = 2.5$ GPa
Radius (m)	17.5	Poisson's Ratio	$\nu = 0.34$
Center Rise Height (m)	2.805	Thermal Expansion Coefficient	α_{CTE} =20 ppm/K
Thickness (μm)	50	Yield Stress	$\sigma_y = 172$ MPa

Table 2: PVDF actuator properties.

Patch Properties (PVDF)	
Density	$\rho_p = 1780$ kg/m^3
Elastic Modulus	$E_p = 2.27$ GPa
Poisson's Ratio	$\nu_p = 0.225$
Thickness	$h_p = 27$ μm
Piezoelectric Strain Constants	d_{31}= 15x10^{-12} m/V, d_{32} = 4x10^{-12} m/V
Coercive Field Strength	E_{pole} = 80x10^6 Volts
Max allowable voltage	V_{max} = 1620 Volts

Table 3: Other parameters

Parameter	Value
Earth nominal temperature, $T_{nom\text{-}earth}$	298 K
Space nominal temperature, $T_{nom\text{-}space}$	120 K
Initial centre rise height, z_o	2.6 m
Desired centre rise height, z_r	2.8 m
Change in rise height, $\Delta z = z_r - z_o$	0.2 m
Inflation pressure P	24.6 Pa
Membrane pre-stress, $\sigma_{pre\text{-}stress}$	13.8 MPa

Shape correction performance of the PVDF patch actuators is gauged in terms of the RMS error, w_{RMS}. Figure 3 shows the surface deformations and voltages for a 6 °K uniform plus a 6 °K gradient thermal disturbance. Electrical field of some actuators were saturated (control commands exceeded the limits). Without control, the surface RMS error was 4.3 mm. With control, the surface RMS error was 0.19 mm. For this case, 95.58% of the surface error was recovered by the control system.

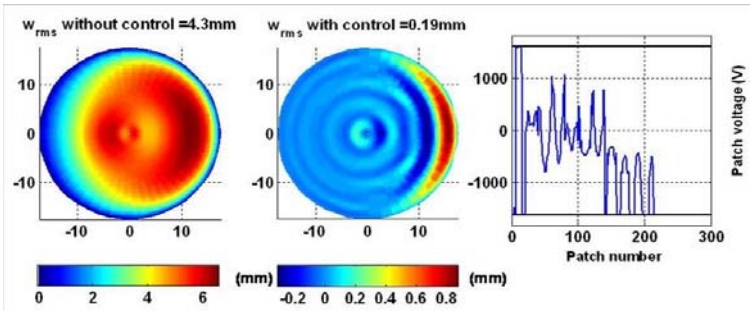

Figure 3. Reflector surface deformations due to 6 K uniform plus a 6 °K

Figure 4 demonstrates the surface deformations and voltages for W-error disturbance with the center rise distance $\Delta z = 0.2$ m. Voltages of all actuators were lower than the saturation voltage. Without control, the surface RMS error was 2 mm. With control, the surface RMS error was 0.0062 mm. For this case, 99.69% of the surface

error was recovered by the control system.

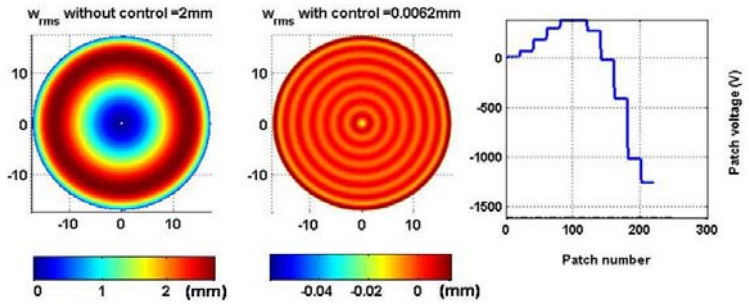

Figure 4. Reflector surface deformations due to W-error (Δz = 0.2m)

From the above preliminary case studies, it can be concluded that this high-precision in-space membrane reflector surface control system with PVDF actuator can be effective for correcting various types of errors and in-space disturbances.

3 DEVELOPMENT OF PVDF BASED ACTUATORS

3.1 Design and fabrication of PVDF actuators

In the reflector shape control system the piezoelectric PVDF films are bonded to passive substrates, resembling the configuration of unimorph bending actuators [3]. In this study, we have developed a process for fabrication and bonding of PVDF films. In order to evaluate the performance of the unimorph actuators, several 1-D beam specimens were tested and compared to theoretical calculations.

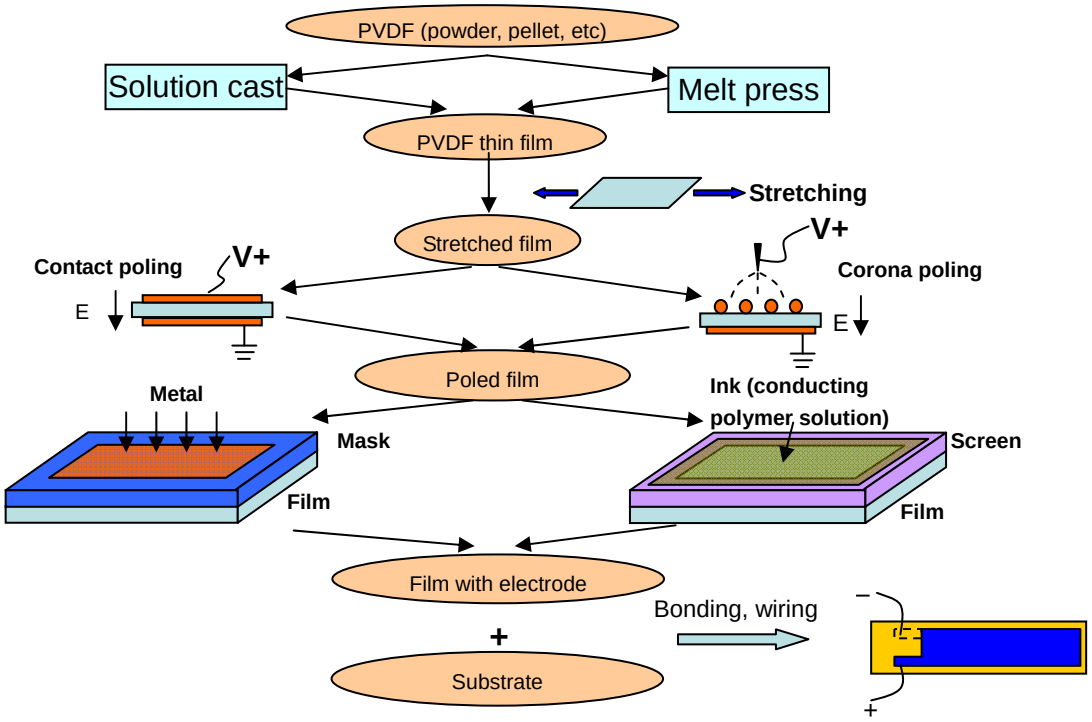

Figure 5. Fabrication process of the 1-D beam specimen.

In general, the fabrication process consists of film preparation, stretching, poling, electrode deposition, and wiring (Figure 5). PVDF thin films are prepared by either casting polymer solution on substrates or pressing polymer melts using heated plates. The films are then stretched to several times along one direction. Poling can be done by contact poling where electric field is directly applied across the film through two contact electrodes. Corona poling is an alternative poling method [4]. In corona poling, film has electrode on only one side and a sharp needle is placed at a certain distance away from the other side. When very high voltage is applied between the needle and the bottom electrode, air ionization happens around the needle and the generated charges accumulate on the film surface, establishing a poling electric field in the film. The poled films are coated with metal or conducting polymer electrodes. Metal electrodes such as silver and gold are deposited by sputtering or thermal evaporation, while conducting polymers can be deposited by screen printing. Compared to the vacuum deposition systems required for metal electrodes, screen printing equipments are much less expensive and can be easily scaled up, and hence the conducting polymer is especially attractive as electrodes for large scale films. The PVDF films can be bonded to substrates using epoxy. By properly selecting the viscosity the epoxy layer can be readily thinned to below 1μm.

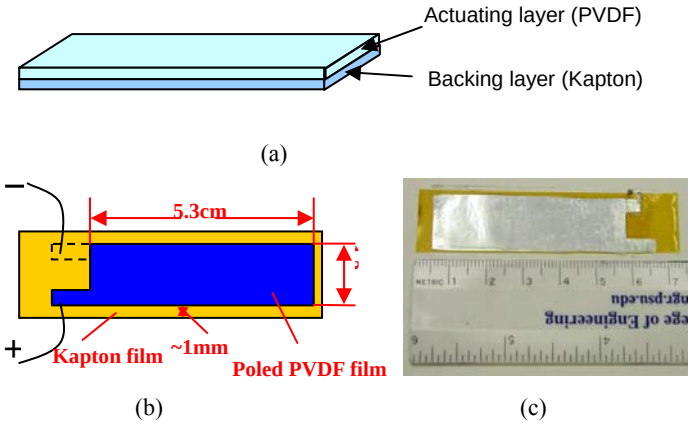

Figure 6. (a) Structure, (b) design, and (c) picture of the testing actuator

Piezoelectric properties of PVDF films were tested using a home built setup [5]. The piezoelectric constants of the PVDF films poled at different temperatures and using different poling methods are listed in Table 4. It was found that corona poling resulted in better piezoelectric properties and film qualities.

Table 4: Piezoelectric constants with different temperatures and poling methods.

Film Source	Poling Method	Poling Temperature	d_{31}(pm/V)
Homemade	Contact Poling	100°C	15
Commercial	Contact Poling	100°C	15
Commercial	Corona Poling	N/A	21.3

We have fabricated 1-D beam actuators by bonding PVDF films to Kapton films (Figure 6). PVDF films were poled at 100°C using contact poling. Both PVDF and Kapton films were 25μm thick. The actuators were tested by observing the tip displacement under different electric fields. The general result was that a 5cm long actuator generated tip displacement of about 1cm under electric field of 40MV/m.

In order to evaluate the performance of the 1-D beams as well as to guide the design of future actuators, we performed theoretical calculation of the tip displacement (d) of the actuators using 1-D unimorph actuator models [6]:

$$\delta = \frac{3d_{31}s_{11}^{k}s_{11}^{p}h_k\left(h_p + h_k\right)L^2V}{K} \tag{1}$$

$$K = \left(s_{11}^{k}\right)^2\left(h_p\right)^4 + 4s_{11}^{k}s_{11}^{p}h_k\left(h_p\right)^3 + 6s_{11}^{k}s_{11}^{p}\left(h_k\right)^2\left(h_p\right)^2 + 4s_{11}^{k}s_{11}^{p}h_p\left(h_k\right)^3 + \left(s_{11}^{p}\right)^2\left(h_k\right)^4 \tag{2}$$

Here s_{11}^{k} and s_{11}^{p} are the elastic compliances at constant electric field of Kapton and PVDF films, h_k, h_p are the thicknesses of the Kapton and PVDF films, V is the applied voltage, and L is the length of the actuator. The

parameters used in the calculation are listed in Table 5. The calculated tip displacements with different PVDF and Kapton thicknesses are shown in Figure 7. The experimentally measured displacement (1cm) is smaller than the calculated value (2.5cm), possibly due to errors in material properties and film geometries, residual stresses in the PVDF films due to poling, the existence of epoxy layer, insufficient control of test environment, and etc.

Table 5: Parameters used in the calculations for PVDF actuators.

Parameter	Description	Value
δ	Tip displacement	--
V	Applied voltage	1000 V
s_{11}^p	Compliance of PVDF	3.1×10^{-10}
s_{11}^k	Compliance of Kapton	4×10^{-10}
t_p	Thickness of PVDF	25μm
t_k	Thickness of Kapton	25μm
d_{31}	Piezoelectric coefficient of PVDF	15pC/N
L	Length	5cm

3.2 Analysis of actuators based on novel electroactive copolymer and terpolymer

Recently, new electroactive polymers have been developed which can achieve much higher strain levels than PVDF. For example, the poly(vinylidene fluoride – hexafluoropropylene) copolymer, P(VDF-HFP), has a large piezoelectric constant of d_{31}=47pm/V. On the other hand, relaxor ferroelectric terpolymer poly(vinylidene fluoride – trifluroethylene – chlorofluoroethylene), P(VDF-TrFE-CFE), exhibits an electrostriction induced strain of as high as 5%, which is almost 100 times larger than PVDF [7,8]. Polymer blend based on P(VDF-TrFE-CFE) terpolymer has Young's modulus several times larger than the pure terpolymer and has similar strain response [9]. These novel materials are promising for achieving more authority in the shape control system. In this study we calculated the tip displacements of actuators based on P(VDF-HFP) copolymer and P(VDF-TrFE-CFE) terpolymer blend using 1-D beam models. The material properties used in the calculations are summarized in Table 6.

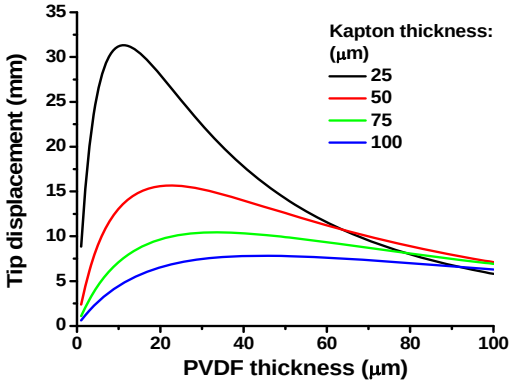

Figure 7. Calculated tip displacement of 1-D unimorph actuator under electric field of

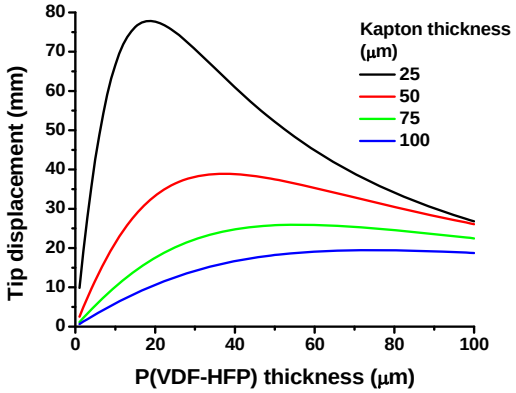

Figure 8. Tip displacement of P(VDF-HFP) unimorph actuators.

The tip displacements of P(VDF-HFP) actuators are shown in Figure 8. It can be found that even though the Young's modulus of P(VDF-HFP) is lower than PVDF, the large piezoelectric constant results in better actuator performances. It should be noted that the large displacements exceeding the length of the actuators are not realistic. In fact, they correspond to the cases where the actuators significantly curl. We calculated the tip displacement for

comparing the performances of different materials rather than predicting the real displacement.

Table 6: Properties of P(VDF-HFP) copolymer and blend based on P(VDF-TrFE-CFE) terpolymer.

Material	P(VDF-HFP)	Terpolymer blend
d_{31}(pC/N):	47	About 3% strain @ 80V/μm
Young's modulus	1GPa	600MPa

It can be expected that P(VDF-TrFE-CFE) based blend should provide much larger tip displacement due to its extremely large electrostrictive strain. However, electrostriction only provide positive strains and hence unimorph actuators based on the structure shown in Figure 6 can only bend toward one direction. In order to realize bi-directional bending we propose a three layer structure where two electrostrictive layers actuate independently (Figure 9). The tip displacement of the three layer actuator is shown in Figure 10. It was found that when proper thicknesses of the active layers were adopted, the bending towards one direction can be one to two orders larger than the piezoelectric polymers, while the bending towards the other direction is of the same level as PVDF actuators.

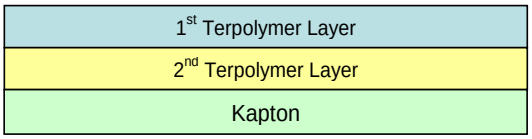

Figure 9. Cross-section of a three-layer beam model.

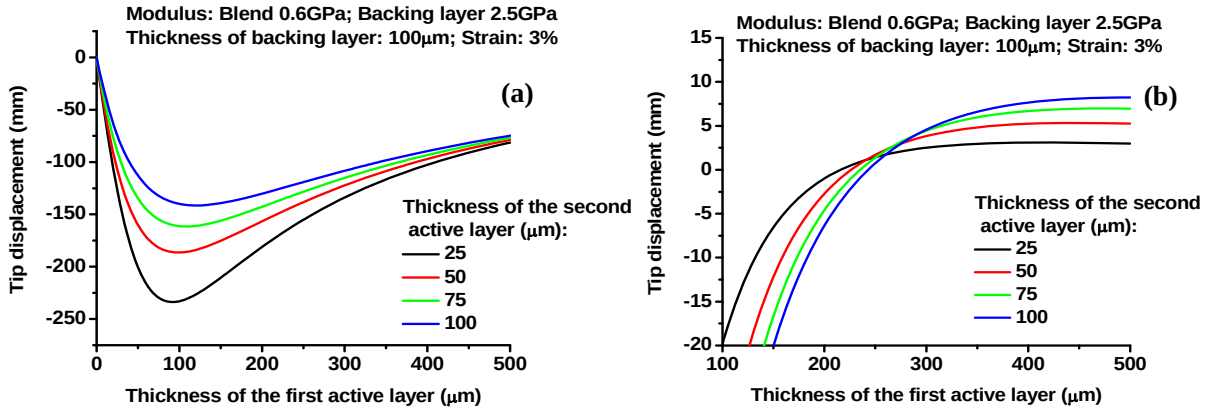

Figure 10. Tip displacements of unimorph actuators based on terpolymer blends. (a) First layer actuating. (b) Second layer actuating.

4 DEMONSTRATION OF MEMBRANE REFLECTOR

In order to demonstrate the feasibility of this innovative reflector surface figure control system, a 0.2-meter diameter membrane reflector engineering model has been assembled and tested. The PVDF films used for this model were obtained from KTech company and were corona poled. In order to increase the actuation authority, double layer actuators (2x25μm) have been fabricated, where the poling direction of the two films were aligned to the same direction and the electrodes were connected so that opposite electric fields were applied on the two films. To implement the PVDF films on the thin-membrane reflector, a mold has been designed and fabricated for attaching actuators to the reflector. The prototype reflector with actuators is shown in Figure 11. The deformation of reflector under applied electric field was measured using a test system which includes the laser metrology unit, digital readout, the power supply, and the test reflector (Figure 12).

Simulations of this reflector prototype were performed with both analytical model (has been discussed in section 2 of this paper) and finite element method (FEM) using properties for the reflector and patch listed in Tables

7 and 8. Under applied field of 1600V, the maximum displace calculated by analytical method was 64.0 μm and the maximum displace calculated by finite element method was 61.3 μm. Both methods correlated with each other very well, which verifies the validity of the analytical model presented in section 2.

Table 7: Reflector Properties.

Radius of Curvature, R	0.28 m
Planform Radius, a	0.1 m
Center Rise Height, z_r	1.85 cm
Thickness, h_{ref}	127μm
Elastic Modulus, $E_{Young's}$	2.5 GPa
Poisson's Ratio, ν	0.33

Table 8: Patch Properties (PVDF).

Density, ρ_p	1780 kg/m^3
Elastic Modulus, E_p	3.2 GPA
Poisson's Ratio, ν_p	0.34
Thickness, h_p	27 μm
Piezoelectric Strain Constants:	d_{31}=22.8x10^{-12} m/V, d_{32}=-4x10^{-12} m/V

The deformation of the reflector was measured with 800V voltage applied. Table 9 shows the measured displacement as well as the displacement calculated using FEM for each point. It can be found that the average of difference is -0.0008 mm and the RMS of difference is 0.0066 mm. The test results showed that the PVDF actuators as developed appear to achieve the required actuations. Possible causes of the differences between the analytical and measurement results include uncertainty of actuator's piezoelectric constants, variation of actuator's geometry dimensions, dimples on the reflector and reflector contour distortion due to mishandling, uncertainty of adhesive effects, mismatch between the analytical model and the test model, pre-strain introduced by bonding flat actuators to a curved reflector, test environment limitation, imperfection of test boundary condition, interferences introduced by wires, and etc.

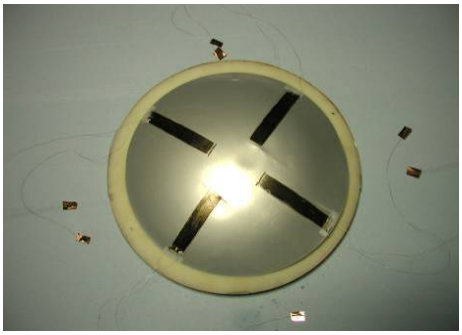

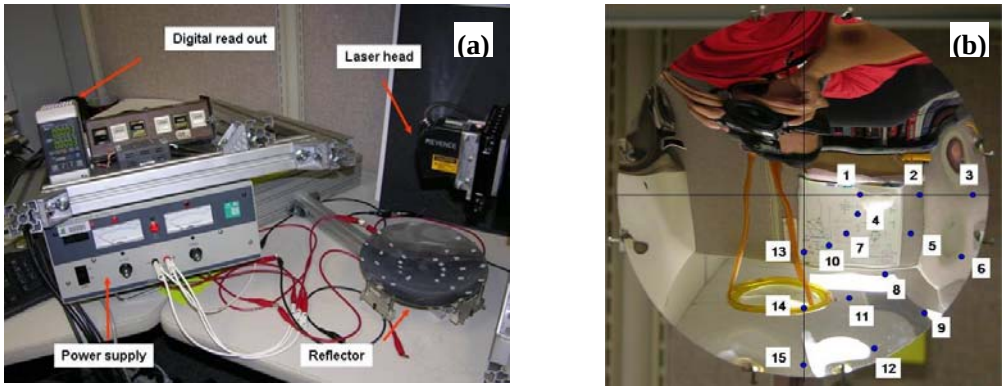

Figure 12.(a)Test set up for measuring the reflector deformation. (b) The reflecting side with test positions labeled.

Table 9: Analyzed and tested displacements (d_{31}= 22.8 x 10^{-12}m/V).

Point	FEA (mm)	Test (mm)	Difference (mm)
1	0.026	0.030	-0.004
2	0.030	0.035	-0.005
3	0.001	-0.004	0.005
4	-0.005	-0.010	0.005
5	-0.006	-0.006	0.000
6	0.008	0.003	0.005
7	-0.002	0.000	-0.002
8	-0.006	-0.002	-0.004
9	-0.021	-0.003	-0.018
10	-0.005	-0.005	0.000
11	-0.006	-0.002	-0.004
12	0.008	0.000	0.008
13	0.026	0.026	0.000
14	0.030	0.038	-0.008
15	0.001	-0.007	0.008

5 CONCLUSION

In this study, we successfully established an analytical model of the system illustrated in Figure 1. The structural part of this analytical model has been verified by the finite element analysis. This analytical model also has been used to investigate the control authority of the system for a 35-m diameter membrane reflector. It has been demonstrated by this analytical model that the proposed control system is capable to control W-shape error, in-space uniform temperature shifting, and in-space gradient temperature loading. We also successfully developed the Flexible PVDF Film actuator technology. To physically demonstrate the feasibility of this innovative control system, a 0.2-meter diameter membrane reflector engineering model has been fabricated and tested. It can be concluded by the analysis and test results of this study that using this innovative high-precision adaptive reflector surface contour control system for ultra-large deployable thin-material antenna reflectors is highly feasible.

ACKNOWLEDGEMENTS

The authors wish to thank Prof. James West in Johns Hopkins university for his help in performing corona poling. PVDF films were purchased from K-Tech Cop.. This work was supported by NASA.

REFERENCES

1. M. Pattom, *High precision shape control of large, light weight space reflectors***,** M.S. thesis, Pennsylvania State University, University Park (2006)
2. H. Hencky, "Uber den spannungszustand in kreisrunden platten," *Z. Math. Phys*., 63, 311-317 (1915)
3. Q. –M. Wang, *Piezoelectric ceramic actuators and composite structure for active noise control applications***,** Ph.D. thesis, Pennsylvania State University, University Park (1998)
4. T. Kaura, R. Nath, and M. M. Perlman, **"**Simultaneous stretching and corona poling of PVDF films", *J. Phys. D.*, 1848-1852 (1991)
5. Z. –Y. Cheng, T. –B. Xu, V. Bharti, S. Wang, and Q. –M. Zhang, "Transverse strain responses in the electrostrictive poly(vinylidene fluoride-trifluoroethylene) copolymer", *Appl. Phys. Lett.*, **74**, 1901-1903 (1999)

6. Q. –M. Wang, X. –H. Du, B. Xu, and L. E. Cross, "Electrosmechanical Coupling and Output Efficiency of Piezoelectric Bending Actuators", *IEEE Trans. Ultrason. Ferroelect. Freq. Contr.*, **46**, 638-646 (1999)
7. Q. M. Zhang, C. Huang, F. Xia, and J. Su: "Electric EAP" in *Electroactive Polymer (EAP) Actuators as Artificial Muscles (2nd ed)*, Y Bar-Cohen, Eds., 95-151, SPIE Press, Bellingham WA, 2004
8. F. Xia, Z. –Y. Cheng, H. S. Xu, H. –F. Li, Q. –M. Zhang, G. J. Karvanos, R. Y. Ting, G. Abdul-Sedat, and K. D. Belfield, "High electromechanical responses in a poly(vinylidene fluoride – trifluoroethylene – chlorofluoroethylene) terpolymer", *Adv. Maters.*, **14**, 1574-1577 (2002)
9. S. H. Zhang, B. Neese, K. L. Ren, B. J. Chu, and Q. M. Zhang, "Microstructure and electromechanical responses in semicrystalline ferroelectric relaxor polymer blends", *J. Appl. Phys.*, **100**, 044113 (2006)